

# Using a maximum simplicity paleoclimate model to simulate millennial variability during the last four glacial periods

Mark Siddall<sup>a,\*</sup>, Thomas F. Stocker<sup>a,1</sup>, Thomas Blunier<sup>a</sup>, Renato Spahni<sup>a</sup>,  
Jerry F. McManus<sup>b</sup>, Edouard Bard<sup>c</sup>

<sup>a</sup>*Climate and Environmental Physics, University of Bern, Bern, Switzerland*

<sup>b</sup>*Geology and Geophysics, Woods Hole Oceanographic Institution, USA*

<sup>c</sup>*CEREGE, CNRS and Université Aix-Marseille III, Europole de l'Arbois, 13545, Aix-en-Provence Cedex 4, France*

Received 14 June 2005; accepted 18 December 2005

## Abstract

Many studies have documented the existence of millennial-scale variability in the Earth system during the last glacial period. An increasing number of studies document the occurrence of similar millennial variability during glacial periods previous to the last one. Here we use the simplest possible thermal-bipolar seesaw model to consider this variability for the last four glacial periods. We invert this model and use the high-pass filtered Vostok stable isotope records to make a first, tentative, attempt to estimate high-latitude N. Hemisphere temperature variability over the last four glacial periods, beyond the reach of Greenland ice-core records. The model result is compared against the Vostok methane record, which shows rapid variations in parallel to Greenland temperature records during the last glacial period. A further comparison is carried out against the planktonic oxygen isotope of north Atlantic core ODP 980. There is agreement between the records on the existence of similar millennial-scale variability during the last three glacial periods with very similar characteristics to the variability during the last glacial cycle.

© 2006 Elsevier Ltd. All rights reserved.

## 1. Introduction

Attempts to understand the past climate variability and its mechanisms involve workers from many different disciplines and those interested in different time and space scales within those disciplines. The large number of varying approaches is exemplified by the wide variety of work published in this special edition of Quaternary Science Reviews. Each discipline approaches the subject with a different background, often with significant variations in terminology. Central to the understanding of past climates is the term ‘model’, which is used in many contexts within paleoclimate research. Because workers use this term with their own understanding and assumptions with regards to its meaning and context, it is useful to take a step back, and state a benchmark reference for the meaning of this word.

We take the [Oxford \(online\) English Dictionary \(2005\)](#) definition of the term ‘model’ in the scientific sense:

A simplified or idealized description or conception of a particular system, situation, or process, often in mathematical terms, that is put forward as a basis for theoretical or empirical understanding, or for calculations, predictions, etc.; a conceptual or mental representation of something. Frequently used with modifying word.

Other dictionaries present similar definitions, e.g. [Websters online \(2005\)](#). While the term ‘model’ is frequently used as short hand for the more specific ‘numerical finite-difference model’, ‘climate model’, etc., it is important to remind oneself of the significant generality of the term. Especially we have to remind ourselves that we are often dealing with models when we still feel we are working with data. When we start to consider data as a proxy for something else, e.g. oxygen isotope values as a proxy for temperature, the proxy is an approximate, or substitute, representation of

\*Corresponding author. Tel.: +41 31 631 4871; fax: +41 31 631 8742.

E-mail address: [siddall@climate.unibe.ch](mailto:siddall@climate.unibe.ch) (M. Siddall).

<sup>1</sup>Also at: International Pacific Research Center, University of Hawaii, Honolulu, HI 96822, USA.

something more complex and therefore might be described as a model by the general definition given here. The use of many classes of ‘models’ pervades all areas of paleoclimate research. Table 1 summarises examples of the different classes of models.

Often, the term ‘model’ stands in conjunction with the term ‘data’, i.e. information that is derived from measurements. By combining models with data, the goal is to generate genuinely new information that could not be gleaned either from data alone, or from models alone. Paleoclimate research is a particularly good example as data are sparse, and often proxy, so models are invaluable tools to give useful, physical meaning to the proxy. Without such models we would be left with the option of unbounded speculation regarding the mechanisms behind

the fluctuations we observe and measure in paleoclimatic data. On the other hand, the construction and application of models without data, against which their results are critically compared and evaluated, exposed and critically evaluated, remains an undertaking that is remote from useful scientific learning.

No single climate model is able to provide definitive answers to paleoclimatic problems. It is therefore imperative to develop and utilise a hierarchy of climate models, ranging from conceptual, but physically based models, to comprehensive 3-dimensional coupled atmosphere ocean general circulation models of high resolution. For paleoclimate research, models of intermediate complexity have become important tools because with their simplified dynamics and reduced resolution, they permit integrations

Table 1  
The use of models in paleoclimate research

| Description   | Examples  | Reference  |
|---|---|--|
| <b>‘A conceptual or mental representation of something’</b>   |   |  |
| <i>Word/conceptual models</i>   |   |  |
| Prevalent in paleoceanography, often a simplified (sometimes simplistic) explanation of ideas derived from numerical or analytical models           | ‘The see-saw’   | Crowley (1992), Broecker (1998), Stocker (1998), Stocker and Johnsen (2003)  |
|   | ‘The conveyor belt’   | Broecker (1987)  |
| <i>Semi-conceptual</i>  |   |  |
| Fixed sets of rules linking variables   | Sea-ice variability models<br>Threshold models<br>Age/synchronisation models  | Gildor and Tziperman (2000)<br>Paillard and Parrenin (2004)<br>SPECMAP—Imbrie et al. (1984), Blunier and Brook (2001)          |
| <b>‘A basis for ... empirical understanding ..., for calculations’</b>  |   |  |
| <i>Empirical models</i>   |   |  |
| Derived from experimental and statistical analysis. This implies description but not understanding of the system                                    | Scavenging models   | Honeyman et al. (1988)   |
|   | Mg/Ca temperature response models<br>Modern temperature analogues for foram assemblages                                 | Nürnberg (1995)<br>CLIMAP—CLIMAP project members (1984)  |
| <i>Analytical models</i>  |   |  |
| Derived from mathematical analysis of governing equations. Either exact or steady-state solutions are found but the results may still be non-linear | Deep ocean circulation<br>Atmospheric circulation<br>Hydraulic models<br>Geochemical models<br>Isostatic rebound models | Stommel and Arons (1960)<br>Lorenz (1963)<br>Siddall et al. (2003)<br>Bacon and Anderson (1982)<br>Lambeck and Chappell (2001) |
| <i>Box models</i>   |   |  |
| Tracer budgets are found allowing for exchange between well-mixed boxes with differing properties   | Global geochemical models   | Oeschger et al. (1975)   |
|   | Stommel 2-box model   | Stommel (1961)   |
| <i>Numerical models</i>   |   |  |
| When neither steady-state nor exact solutions may be derived analytically the governing equations may be approximated by finite-difference methods  | Simplified—EMICs: Bern 2.5D, Bern 3D  | Stocker et al. (1992), Müller et al. (in press)  |
|   | Detailed—AOGCMs: Hadley Centre model, NCAR’s CCSM<br>Ice-sheet models   | Manabe et al. (1975), Bryan et al. (1975), Johns et al. (2003), Collins et al. (in press)<br>Tarasov and Peltier (2004)        |

This table is not intended to be exhaustive but merely to indicate the diversity of models used in contemporary paleoclimate research. There are many more subcategories and models that could be included here.

covering many millennia. The model-based investigation of long-term climate change is therefore no longer limited to simple conceptual modelling. However, due to the absence, or parameterisation of some key processes, the utilisation of models of intermediate complexity requires thorough testing of parameter ranges and comparison with more complete models (Stocker and Knutti, 2003).

In this paper, we present a simple exercise to combine data with a specific model with the goal generating information that would otherwise not be available. We use probably the simplest mathematical model for millennial-scale climate change, the thermal-bipolar seesaw, which is suitable for the paleoclimate data that we will make use of. With this combination we make a first estimate of the variability of North Atlantic temperature caused by millennial-scale changes during glacial periods. The model is inverted and used to “reconstruct” abrupt change by using as input the deuterium isotope data of the Vostok ice core during glacial periods MIS 10, 8, 6 and 3. This model-generated record is then compared to measurements of methane within the Vostok core and oxygen isotope ratios from North Atlantic core ODP 980.

## 2. The bipolar seesaw model

Blunier et al. (1998) and Blunier and Brook (2001) use the globally well-mixed methane signal in the GRIP and Byrd ice cores as a means to synchronise the two records to a common time frame. The resulting synchronised temperature records show that rapid warmings in Greenland during MIS 3 are timed to the peaks in Antarctic temperature. These rapid warmings occur on millennial time scales and are generally referred to as Dansgaard–Oeschger (D–O) events (Dansgaard et al., 1984, 1993; Oeschger et al., 1984). The rapid warmings are thought to occur following periods of freshwater input into the North Atlantic, which interrupts the transport of heat from lower latitudes by slowing or stopping the ocean thermohaline circulation. Crowley (1992) pointed out that the active thermohaline circulation in the Atlantic Ocean actually cools the southern hemisphere, and Stocker et al. (1992) demonstrated this independently in a climate model of intermediate complexity (their Fig. 11b). The simple concept of the bipolar seesaw (Broecker, 1998; Stocker, 1998) postulated strict anti-phase behaviour between temperatures in the North and the South Atlantic. However, taking the temperature reconstruction based on Antarctic ice cores as a proxy for the South Atlantic temperature suggested a lag-relationship rather than an anti-phase behaviour (Blunier et al., 1998). Several correlation attempts using the reconstructed temperatures from Greenland and Antarctica produced a series of proposals as to how the two hemispheres were coupled. They ranged from lead or lag, to in-phase, out-of-phase, to anti-phase (Bender et al., 1994; Blunier et al., 1997, 1998; Broecker, 1998; Blunier and Brook, 2001; Stocker, 1998; Steig and Alley, 2002; Schmittner et al., 2003).

In this apparent confusion of notions, the introduction of the thermal-bipolar seesaw, a slight extension of the original concept, proved helpful (Stocker and Johnsen, 2003). The temporal behaviour of the south is not in simple correlation to that of the north, but is an integration in time due to the thermal storage effect of the southern ocean. In this concept, the Southern and Northern Atlantic are in anti-phase, whereas the Southern Ocean, and Antarctica by inference, communicate with the South Atlantic through heat transfer. However, while explaining much of the variance, the thermal-bipolar seesaw is not entirely satisfactory because the time scale that characterises the heat transfer is longer than that predicted by dynamical models. This inconsistency was addressed using a 3-dimensional ocean circulation model coupled to a simple atmosphere model (Knutti et al., 2004). These simulations demonstrated that the changes in freshwater had a direct effect on the circulation and hence the south–north heat exchange.

As noted Blunier and Brook (2001) present a highly useful synchronisation of the GRIP and Byrd ice cores. However, a significant limitation of the Greenland ice cores is their reduced length compared to either marine records or Antarctic ice-core records. The maximum age of a Greenland ice core is 123 ka (North GRIP members, 2004). This compares with several million years for ocean sediment cores and ages approaching 1000 ka for Antarctic ice cores (EPICA community members, 2004). Although the Greenland ice-core records have already provided key insights into the Earth’s climate, in particular our understanding of abrupt climate change (e.g. Alley et al., 2003), their major limitation is the lack of Greenland records previous to the last interglacial.

Here we present a first attempt to simulate high-latitude northern hemisphere temperature records from Antarctic temperature records for the last four glacial periods using a ‘maximum simplicity’ model for the seesaw-type variability, thereby overcoming the age limitation of the Greenland ice cores. The approach is based on the ‘minimum complexity’ thermodynamic model for the bipolar seesaw (Stocker and Johnsen, 2003). We use the terms ‘minimum complexity’ and ‘maximum simplicity’ model to denote the simplest possible model that still captures the phasing and magnitude of the Greenland and Antarctic ice-core records. The model is an energy balance of the Southern Ocean; heat transfer is parameterised as proportional to the temperature difference between the Southern Ocean and the South Atlantic. Between the South Atlantic and the North Atlantic, we assume a perfect seesaw. This can be written as

$$\frac{dT_s(t)}{dt} = \frac{1}{\tau}(-T_N(t) - T_S(t)), \quad (1)$$

where  $T_N$  is the temperature of the North Atlantic, and  $T_S$  is the temperature of the Southern Ocean;  $t$  is time and  $\tau$  is a time scale related to the Southern Ocean heat reservoir. Stocker and Johnsen (2003) found a value of  $\tau = 1.12$  ka

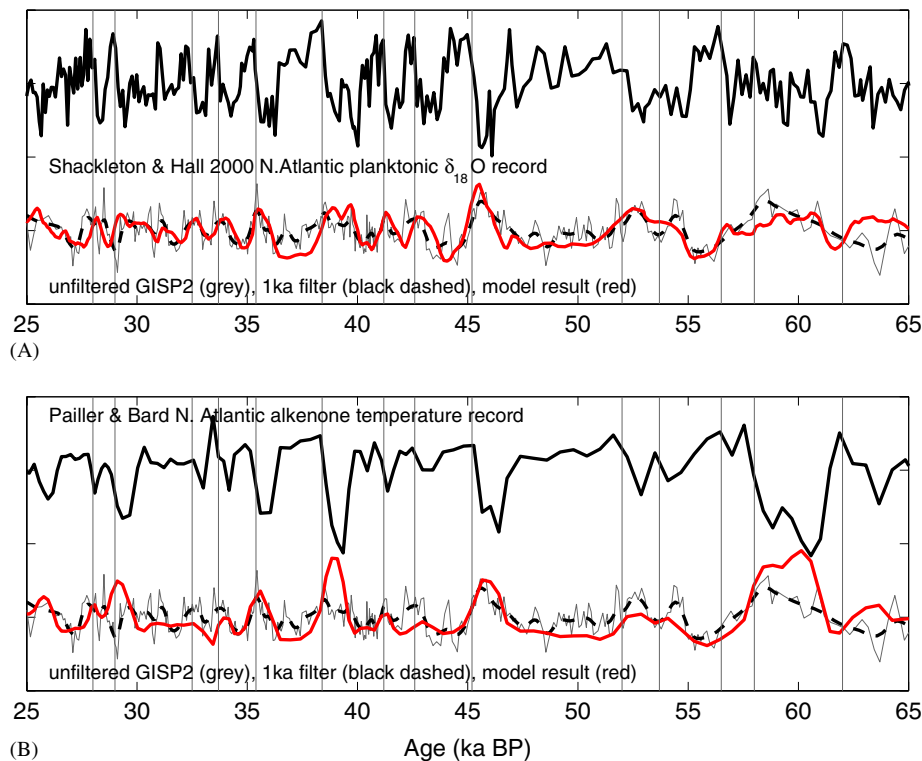


Fig. 1. Application of the original, forward thermal seesaw model to the 8 ka high-pass filtered GISP 2 synchronised from two N. Atlantic temperature proxy records from the Portuguese Margin core MD95-2042: (a)  $\delta^{18}\text{O}$  from *Globigerina Bulloides* samples in core (Shackleton and Hall, 2000) and; (b) the alkenone derived temperature record from (Pailler and Bard, 2002).

that best fitted the GRIP and Byrd ice-core data as synchronised by Blunier and Brook (2001) and could explain nearly 80% of the variability in the Byrd ice core. Such a large value for  $\tau$  is not supported by dynamical models of temperature adjustment in the Southern Ocean. A model of the MIS 3 bipolar seesaw including freshwater forcing shows lower values of  $\tau$  (0.12 ka, Knutti et al., 2004). However, here we are considering earlier isotope stages, for which detailed sea-level histories do not exist. Therefore we use the simpler, thermal-bipolar seesaw model, which has been shown to adequately represent the ice-core data within the scope of this exercise.

### 2.1. Testing the robustness of the standard thermal-bipolar seesaw model to different input data

Stocker and Johnsen (2003) demonstrated the thermal-bipolar seesaw model simulates Antarctic temperatures if forced with temperature records from the GRIP ice core. To increase our confidence in the ability of the standard (forward) thermal-bipolar seesaw model to simulate Antarctic temperature records we test it using a variety of input temperature records from a variety of proxies and locations. Fig. 1 shows this result from two N. Atlantic temperature proxy records from the Portuguese Margin core MD95-2042:  $\delta^{18}\text{O}$  from *Globigerina bulloides* samples (Shackleton and Hall, 2000) and; the alkenone derived temperature record from (Pailler and Bard, 2002). It is

particularly interesting to make use of a N. Atlantic alkenone-temperature record which show close similarity to 'Heinrich event'<sup>2</sup> in the same cores (Bard et al., 2000; Pailler and Bard, 2002; Bard, 2002). In contrast, the cold periods relating to iceberg-rafting events are relatively subdued in Greenland records when compared to D-O events. We note that  $\delta^{18}\text{O}$  from *Globigerina bulloides* samples is not a pure SST signal but also contains components linked to variations in global ice volume and local hydrological conditions, which were probably very large, especially during 'Heinrich events'.

Although there are limited differences resulting from differences in the input data, there are strong similarities in the amplitude and phase of the simulated Antarctic temperatures. An interesting feature is that the Antarctic warm events corresponding to 'Heinrich' events are somewhat larger when using the N. Atlantic Sea Surface Temperature record rather than Greenland temperatures. These comparisons give us enough confidence in the ability of the thermal-bipolar seesaw model to simulate Antarctic temperature with a variety of input data for us to attempt to apply an inverted version of the model to records of Antarctic temperature.

<sup>2</sup>Here we use the term 'Heinrich event' to denote 'iceberg-rafted debris events'. Precise definitions of 'Heinrich events' vary, see Hemming (2004) for a thorough review.

## 2.2. The inverse bipolar seesaw model

The simplicity of Eq. (1) means that it may easily be rearranged to give the high-latitude northern temperatures as a function of Antarctic temperature and its changes:

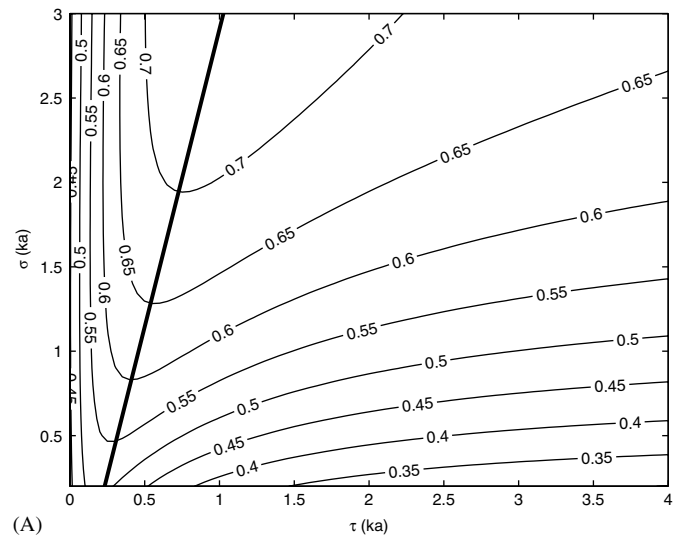
$$T_N(t) = -T_S(t) - \tau \frac{dT_S(t)}{dt}. \quad (2)$$

This turns out to be a useful tool since, as already noted, Greenland ice cores are many times younger than their southern counterparts. Eq. (2) opens up the possibility of simulating high-latitude northern temperatures as a function of Antarctic temperature during periods of high-amplitude millennial-scale variability (i.e. the glacial stages) which predate the oldest Greenland ice-core records. Eq. (2) is therefore considered a *proxy model* for Greenland temperature.

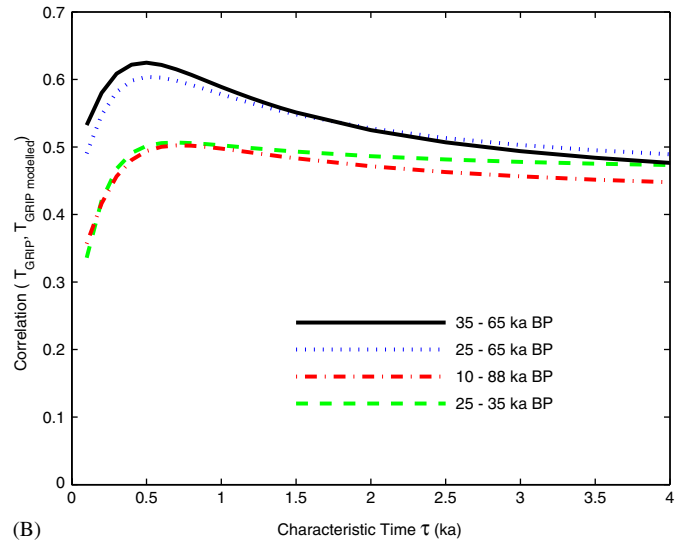
## 3. Demonstration of the inverse bipolar seesaw for MIS 3

A high-pass gaussian filter with a cut off at 8000 years is used to remove the long-term insolation driven signal in Antarctic temperature from Byrd for MIS 3 and from Vostok for MIS 3, 6, 8 and 10. Applying a simple centred difference scheme to the filtered Byrd temperature record Eq. (2) is then used to generate an approximation for the time series of northern hemisphere temperature for signals with periods between 1500 and 8000 years. An immediate problem arises in that noise in the Antarctic records is magnified by the finite-difference scheme. In the original forward calculation (calculating Antarctic temperature from Greenland records) the integration of northern temperature over the time  $\tau$  removes noise. Applying a low-pass gaussian filter to the Antarctic records before taking their derivatives removes the problem of this noise but effectively adds another variable to the calculation—the length of the filter window,  $\sigma$ . Because varying  $\sigma$  changes the derivative of the Antarctic record, for each value of  $\sigma$  there is a different optimal value for  $\tau$  (Eq. (1)). The relationship between  $\sigma$ ,  $\tau$  and the best fit to data is shown in Fig. 2a for the period 65–35 ka BP. Since we are interested in signals with intervals of around 1.5 ka (Dansgaard et al., 1993) a value for  $\sigma$  of 1 ka is adequate to remove noise and sub-millennial variability in the Antarctic records. We have repeated this exercise for a variety of filter types (band-pass and digital filters) with the outcome that this result is robust to the type of filter chosen.

Stocker and Johnsen (2003) calculate correlation coefficients for different values of  $\tau$  and for different periods (MIS 3, MIS 5 to MIS 1, etc.). We repeat this process here for the last glacial cycle for our inverted method (Fig. 2b). For the period when the model performance is at an optimum the model gives a correlation coefficient of 0.63, indicating that it is representing 80% of the variability in the high-latitude N. Atlantic. Stocker and Johnsen (2003) found an optimal value for  $\tau$  of 1.12 ka. Here we find a



(A)



(B)

Fig. 2. The correlation coefficient between the 8 ka high-pass filtered GRIP record and the model output. The optimal correlation is achieved for different values of  $\tau$  with different  $\sigma$  values as is shown by the contours of the correlation coefficient for the period 65–35 ka BP in (a) with the line of optimal fit also shown. The glacial periods show markedly better agreement between model and data, indicating that the model is not valid for major interglacials as shown by (b) where  $\sigma$  is 1 ka.

value of 0.5 ka gives the best fit to data with a value for  $\sigma$  of 1 ka. A simple visual comparison of the model results in Fig. 3a seems to indicate that a value for  $\tau$  of 1.12 ka simulates best the magnitude of the variation during the period from 48 to 28 ka BP but gives unrealistic variability during other periods. The correlation coefficient takes the whole period into account and during earlier parts of the record (60–45 ka BP) a  $\tau$  of 0.5 ka gives a better visual fit. Overall a  $\tau$  of 0.5 ka gives a better fit. Given the simplicity of our approach there is reasonable similarity between the reversed and original thermal seesaw calculations. Simulations for both  $\tau = 0.5$  ka and  $\tau = 1.12$  ka shown in Fig. 3 vary only slightly from each other. Fig. 2 shows that the correlation coefficient for  $\tau = 1.12$  ka is similar to that for

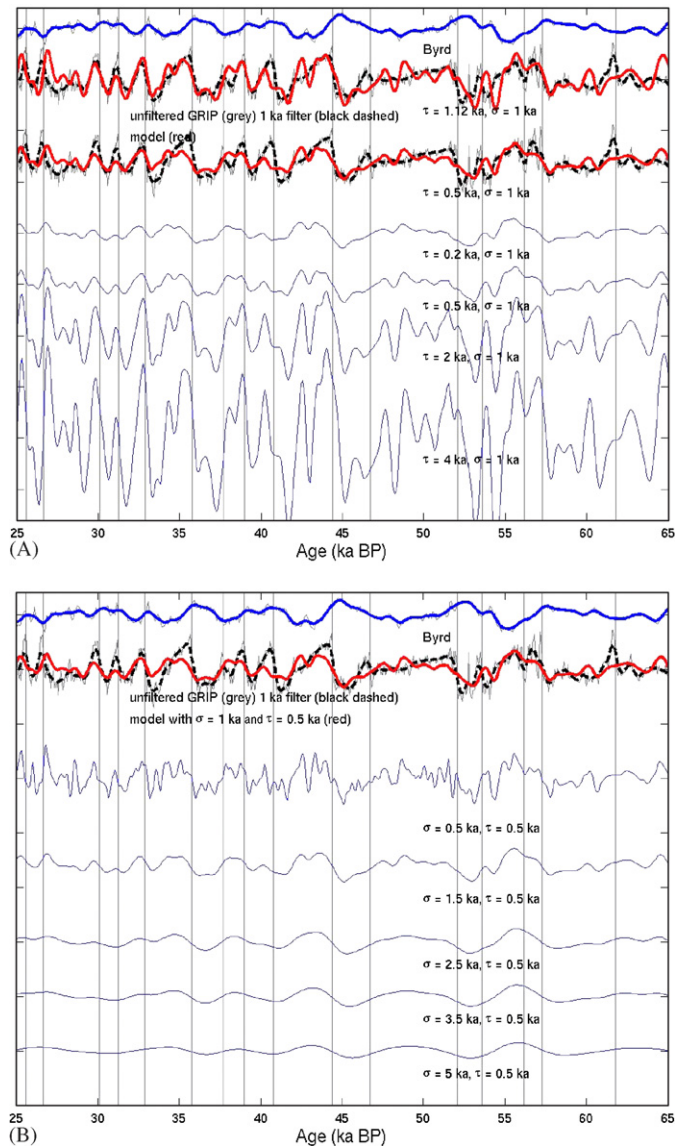


Fig. 3. Application of the model to the 8 ka high-pass filtered Byrd and GRIP methane-synchronised  $\delta^{18}\text{O}$  records for various values of (a) the characteristic age,  $\tau$  (keeping  $\sigma$  constant at 1 ka) and (b) the low-pass filter length,  $\sigma$ , used to remove high-frequency noise (keeping  $\tau$  constant at 0.5 ka). Vertical grey lines indicate D–O events.

$\tau = 0.5$  ka for the period 65–25 ka BP. We are therefore confident in using a  $\tau$  value of 0.5 ka in the rest of the paper. The resulting signal for MIS 3 is shown in Fig. 3 for several values of  $\tau$  and  $\sigma$ . The comparison between the simulated and observed high-latitude northern temperatures is good. The major D–O events are all simulated.

Seesaw-type millennial-scale variability is thought to be forced by periodic freshwater release at high-northern latitudes in the Atlantic (e.g. Knutti et al., 2004). Such freshwater release is likely related to the instability of large ice sheets during the glacial periods. During periods of reduced ice volume (interglacials) the model performs less well (Fig. 2b, Stocker and Johnsen, 2003). One may conclude that seesaw-type variability is less dominant

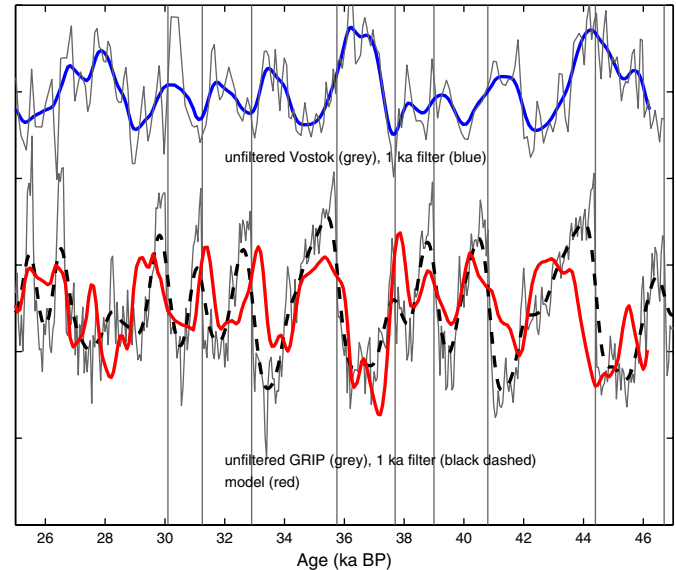


Fig. 4. Application of the model to the 8 ka high-pass filtered and methane-synchronised Vostok deuterium and GRIP  $\delta^{18}\text{O}$  records for MIS 3. For the calculation shown  $\sigma$  is 1 ka and  $\tau$  is 0.5 ka. The Vostok deuterium record has been reduced by a factor of eight to give it comparable magnitude to the GRIP  $\delta^{18}\text{O}$  record. Vertical grey lines indicate D–O events.

during times of reduced ice volume, although millennial-scale variability may exist during these periods (e.g. Rohling and Palike, 2005). This conclusion is in agreement with the detailed analysis of millennial-scale variability since MIS 13 presented by McManus et al. (1999), which finds an absence of IRD events and large amplitude millennial variability during the interglacials. Therefore, in considering previous glacial periods we take periods between the major interglacials to apply the method.

Blunier et al. (1998) provide a synchronisation of the GRIP and Vostok ice cores based on methane concentration for the last 46 ka. This allows us to test the validity of the reverse see saw method during MIS 3 using the Vostok deuterium record as a high-latitude southern hemisphere temperature record. The results from this calculation are shown in Fig. 4 where they are compared with the GRIP  $\delta^{18}\text{O}$  record. Values of  $\tau = 0.5$  ka and  $\sigma = 1$  ka are taken from the best-fit scenarios described earlier in the text. The result compares well to that achieved using the Byrd record and discussed earlier. This gives us some confidence in applying the method to MIS during glacial periods since MIS 8 using the Vostok deuterium record to drive the model.

#### 4. A first attempt to reconstruct Greenland temperature before 123 ka BP

During MIS 3 synchronised Greenland and Antarctic records allow the sort of analysis presented by Stocker and Johnsen (2003) and reproduced here for the inverse-seesaw model. However, such records do not exist for previous glacial stages due to the reduced length of the Greenland

ice record, and options as to the choice of data with which to compare the model result is limited. The methane record is considered to be an imperfect but close proxy for northern hemisphere temperatures on millennial time scales (Chappellaz et al., 1993; Petit et al., 1999; Blunier and Brook, 2001; Delmotte et al., 2004) during MIS 3. We assume that this relationship is also maintained during MIS 6, 8 and 10 and compare the model results to the methane record for these periods. We further assume that the ice age to gas age difference ( $\Delta$ age) has been accurately taken into account, and that the CH<sub>4</sub> signal attenuation (Spahni et al., 2003) is of minor importance here.  $\Delta$ age models are sensitive to their input parameters and therefore uncertainty in  $\Delta$ age is relatively large, especially during glacial periods (e.g. Delmotte et al., 2004). Here we use the modelled  $\Delta$ age (GT4–A55) of Delmotte et al. (2004). This  $\Delta$ age model gives a consistent Antarctic warming prior to rapid transitions in the CH<sub>4</sub> record in agreement with evidence for millennial variability during MIS 3.

An alternative is to consider North Atlantic marine cores such as ODP core 980, presented by Oppo et al. (1998) and McManus et al. (1999). The ODP 980 record includes IRD, surface planktonic  $\delta^{18}\text{O}$  and benthic  $\delta^{18}\text{O}$ . Evidence for millennial-scale variability has been identified in this core (Oppo et al., 1998; McManus et al., 1999). Despite the rather low resolution of the Vostok and ODP 980 records there are clear similarities between them in the millennial band, and we use these similarities to synchronise the two records. The synchronisation is based on the characteristic behaviour of multiple proxies during millennial events as outlined in Table 2 and not just similarities between two proxies. Each of the proxy records included in this paper has weaknesses and may not record individual events at the coring locations. By combining multiple proxies in each record and the model results the uncertainty in identifying events in individual proxy records is reduced. Only well-characterised events are used as tie points, and the resulting

synchronised records are shown in Fig. 5. Due to the respective resolution of each core we do not consider this a perfect solution to the problem of synchronisation for high-latitude northern and southern hemisphere records. Here, however, we establish the potential for this approach for application to high-resolution records in the future.



#### 4.1. MIS 6

Fig. 6 shows the comparison between the ODP 980 proxy records, the Vostok records and the model simulation for MIS 6. Comparison with the high-resolution Vostok methane record demonstrates that the model reasonably simulates the high-latitude northern temperatures during this period. The similarities between MIS 3 and MIS 6 are worth mentioning. The period between 180 and 155 ka BP shows a marked similarity to MIS 3 (25–65 ka BP). We further note that the events related to the transitions 5d to 5c, 5b to 5a, 7d to 7c, 7b to 7a also show strong similarities—in each case a gradual southern warming leads the rapid temperature transition in the northern hemisphere (as indicated by the methane record) (Fig. 5). Despite the comparatively low resolution of the ODP 980 record variability with a period of around 7 ka is comparable between the model and the planktonic  $\delta^{18}\text{O}$  record.

#### 4.2. MIS 8

Fig. 7 shows a similar comparison for MIS 8. The comparison between the model simulation and the Vostok methane record is reasonable. On approximately 7 ka time scales the modelled high-latitude north Atlantic temperature captures the major temperature changes indicated by the ODP 980 planktonic  $\delta^{18}\text{O}$  record. The model shows additional variability to that resolved by the Vostok methane and N. Atlantic planktonic  $\delta^{18}\text{O}$  record. It will

Table 2  
Criteria for tie points and model comparison based on millennial-scale variability

| Event   | Antarctic events   | ODP 980  | Model predicted northern temperature  |
|---|--|--|---|
| freshwater discharge  | <i>Warming in progress</i>   | <i>IRD layer</i>   | Cold  |
|  | ----- tie point -----  |  |  |
| end of freshwater discharge   | <i>Temperature maximum</i><br><i>Rapid increase in methane concentration</i> | <i>End of IRD layer</i><br><i>Rapid warming indicated by planktonic <math>\delta^{18}\text{O}</math></i><br><i>Minimum in benthic <math>\delta^{18}\text{O}</math></i> | Rapid cold to warm temperature transition   |

This table indicates ‘typical’ observed and model-predicted responses—it does not indicate exact cause and effect. Time flows from top to bottom of table. The actual responses are not reproducible in all cores and all of these events being recorded in cores for every cycle is not anticipated. Tie points are assigned where the criteria are met for multiple records.

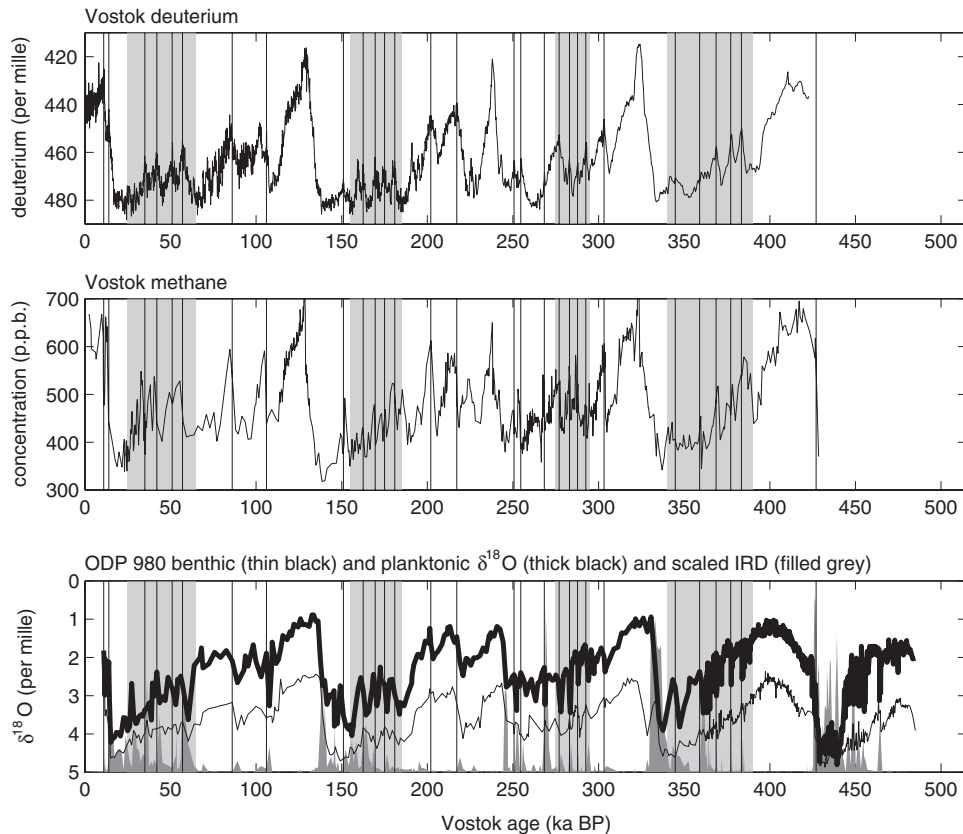


Fig. 5. The synchronised records on a GT4 Vostok time scale using the tie points between the Vostok ice time scale and ODP-980 (vertical black lines). Figs. 1, 3, 4, 6, 7 and 8 cover the events shown in the grey boxes.

be interesting to discover whether this variability is found as alternative, high-resolution records for these periods become available.

#### 4.3. MIS 10

Fig. 8 shows a transition between the high- and low-resolution sampling of ODP 980 during MIS 10. Unfortunately during this period the resolution of the Vostok deuterium record is not comparable to that of ODP 980. Only the larger variations in the northern hemisphere temperatures with a period of around 7 ka are simulated, although these compare well with the planktonic  $\delta^{18}\text{O}$  record. Because of the low resolution of the Vostok record during MIS 10 it is not possible to discern particular periods of the record demonstrating MIS 3-type variability and the whole of MIS 10 is shown. Unlike the other MIS considered here during MIS 10 there is not a clear agreement between the model results and the Vostok  $\text{CH}_4$  record. During much of the MIS 10 record this is due to the comparatively low resolution of the Vostok records. Between 390 and 370 ka BP there appears to be a phase difference between the model result and the methane record, perhaps indicating a problem with the  $\Delta$ age model for this interval. Along with the low-resolution record of Vostok the planktonic  $\delta^{18}\text{O}$  record of ODP 980 indicates

that the most likely period for MIS 3-type variability during MIS 10 is between 360 and 370 ka BP on the Vostok time scale presented here. Higher resolution sampling of Antarctic ice will be needed to confirm this suggestion.

#### 4.4. Statistical comparison of the model simulations with the Vostok methane record

As a test of the capability of the model to simulate high-latitude N. Hemisphere temperature variability during MIS 6, 8 and 10 our only option is to compare the model simulations to the Vostok methane record. In order to make statistical comparisons between the Vostok methane on the GT4–A55 time scale and the model results it is necessary to subsample the model output at the same interval as the Vostok methane record. Because the resolution of the methane record is different from the resolution of the model output (which has the same resolution as the Vostok Deuterium record) there are several stages in this comparison. We first perform a spectral analysis in order to determine the spectral band in which useful information is contained in the Vostok methane record. We then use the spectral analysis to determine an appropriate low-pass filter to apply to the model output (Fig. 9). In this way we ensure that any statistical comparison of the model output and the Vostok



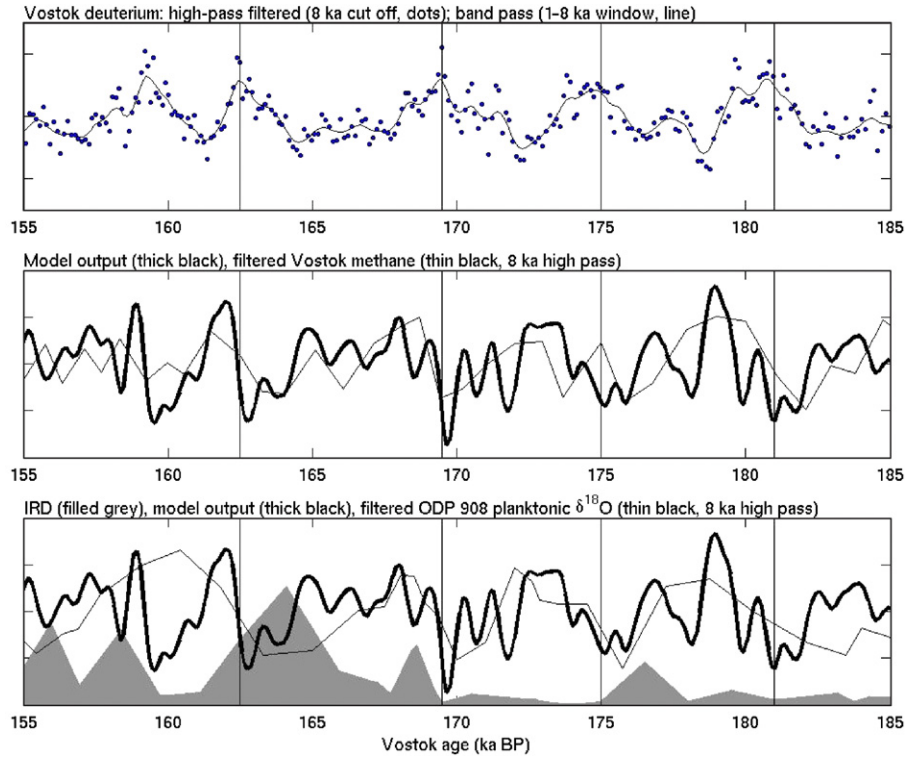


Fig. 6. Applying the model to MIS 6, comparison to other proxies and tie points between the GT4 Vostok ice time scale and ODP-980 (vertical black lines).

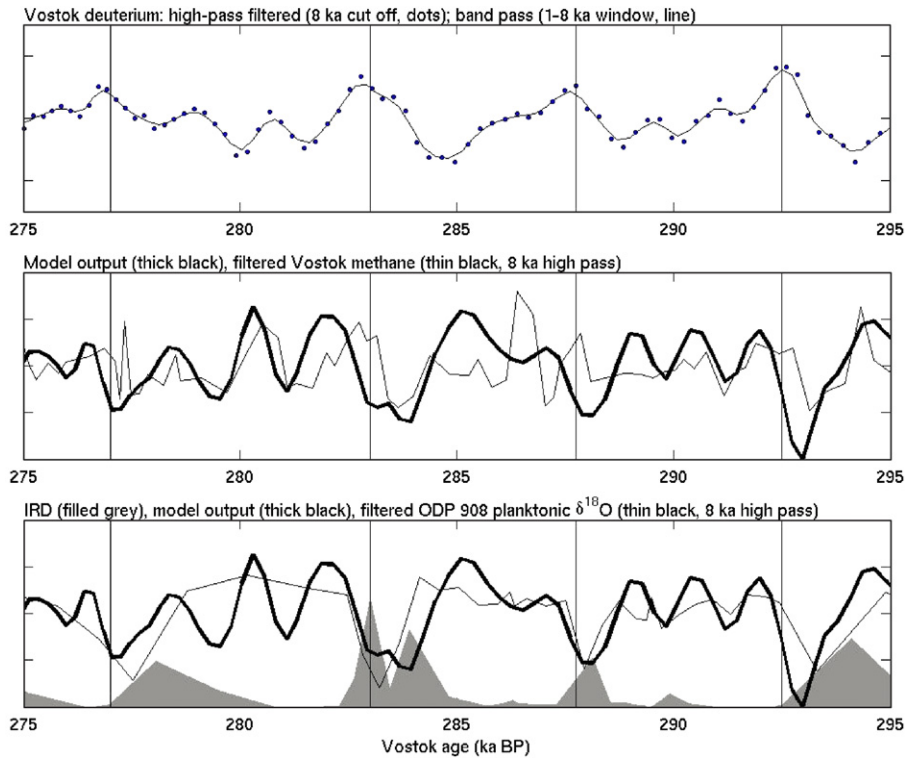


Fig. 7. Applying the model to MIS 8, comparison to other proxies and tie points between the GT4 Vostok ice time scale and ODP-980 (vertical black lines).

methane record is across the appropriate range of frequencies. The low-pass filters derived in this way have window lengths of 2 ka (MIS 6), 1 ka (MIS 8) and 2 ka

(MIS 10). We note that the resolution of the MIS 10 record (~1 ka) is such that there are no strongly dominant peaks in the energy band shown in Fig. 9. As already noted this

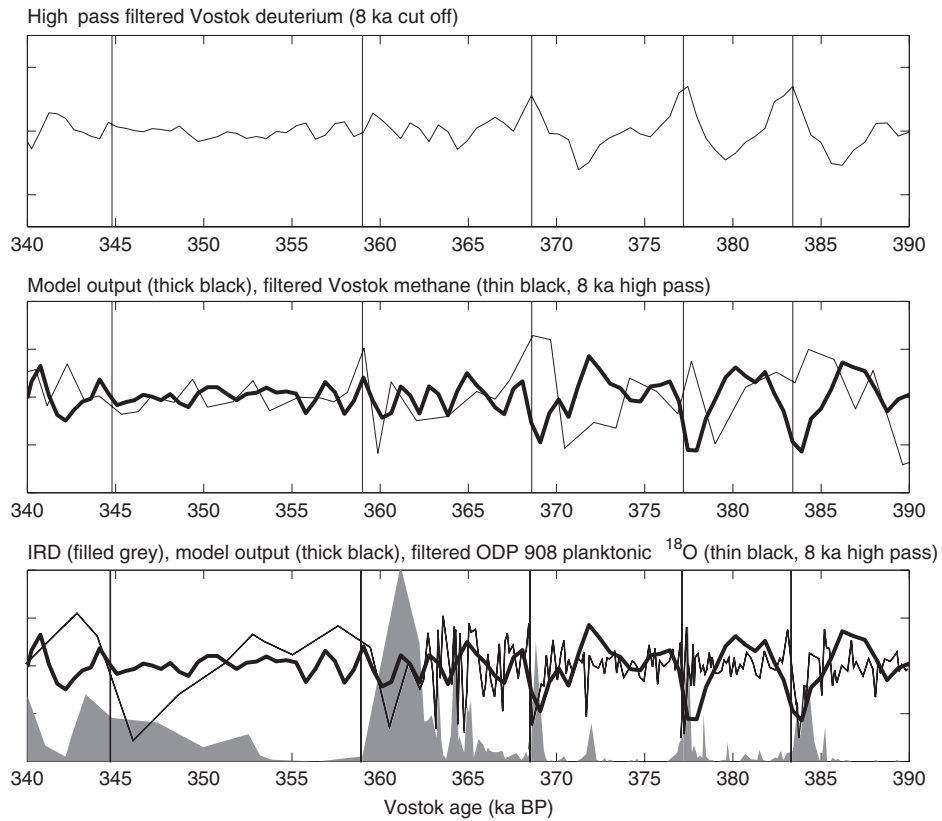


Fig. 8. Applying the model to MIS 10, comparison to other proxies and tie points between the GT4 Vostok ice time scale and ODP-980 (vertical black lines).

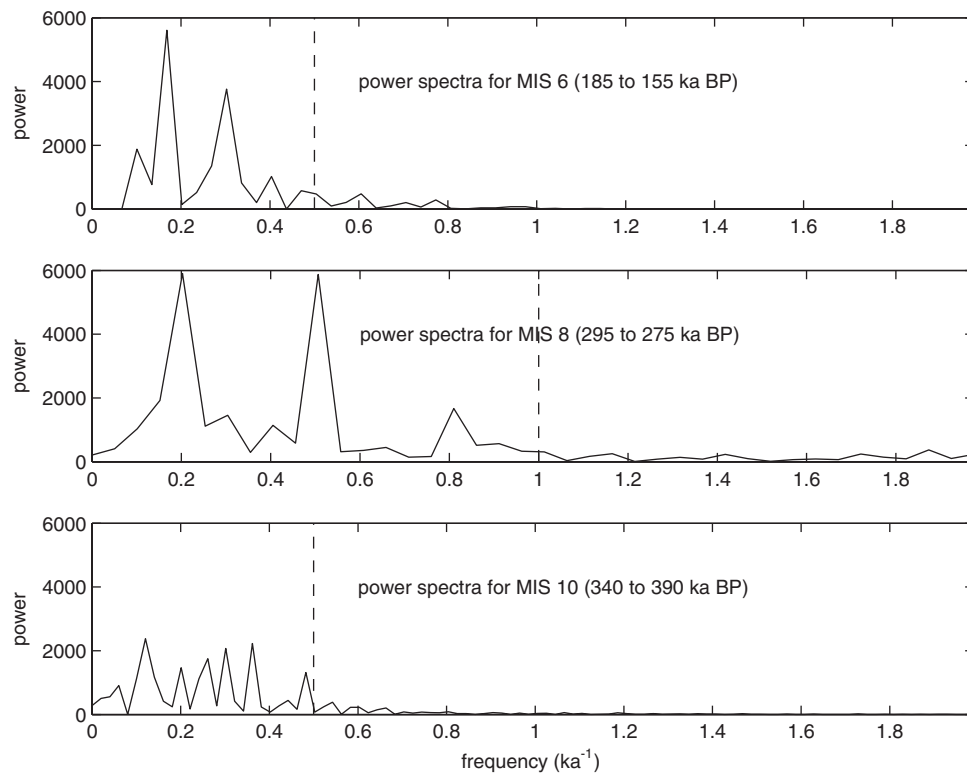


Fig. 9. FFT power spectra for the Vostok methane record on a GT4–A55 time scale (Delmotte et al., 2004) during MIS 6, 8 and 10. The dashed vertical lines indicate the cut off frequency for the analysis presented in Fig. 10 (see text for details).

comparatively low resolution means that the model result for this MIS 10 is not representative of the general ability of the model.

A second issue arises from the uncertainty in the  $\Delta$ age of the methane record (Delmotte et al., 2004). It is therefore necessary to take into account any slight phase offset between the two records. In order to do this we calculate correlation coefficients for the model output and the Vostok methane record while adjusting the age scales of the two records relative to each other to allow for phase differences between the records. Fig. 10 shows the results of this analysis. Only a slight phase shift (0.4 ka) is apparent during MIS 6. Although this is only a slight age offset it is nonetheless important in the calculation of correlation coefficients. The phase shift during MIS 8 is slightly longer at 0.7 ka. For MIS 10 the phase shift is as large as 2 ka but this is not a robust result given the comparatively low resolution of the Vostok deuterium and methane records during this period. These age offsets are well within the differences in  $\Delta$ age between the selection of  $\Delta$ age models presented by Delmotte et al. (2004). Allowing for age offsets the resulting correlation coefficients are 0.57 (MIS 6), 0.42 (MIS 8) and 0.44 (MIS 10). Note that the age offsets calculated here represent constant offsets through each individual MIS. Given that the offsets will vary continuously throughout each MIS the correlation coefficients found here are a lower estimate of how well the model simulates high-latitude northern hemisphere temperatures. Note that methane closely resembles, but it is not identical to, Greenland temperature records during MIS 3 (Chappellaz et al., 1993; Petit et al., 1999; Blunier and Brook, 2001; Delmotte et al., 2004), which also partly explains the slightly low correlation coefficients found here.

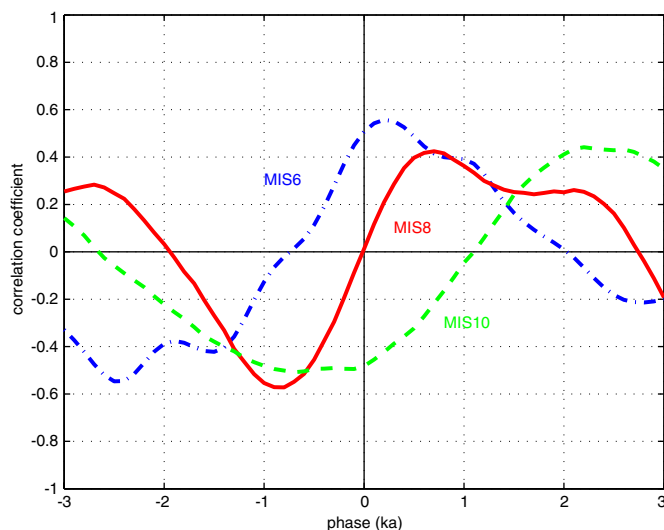


Fig. 10. Phase analysis of the model output versus the Vostok methane records on a GT4–A55 time scale (Delmotte et al., 2004) for MIS 6, 8 and 10. The correlation coefficients are optimised for phase shifts of 0.4 ka (MIS 6), 0.7 ka (MIS 8) and 2 ka (MIS 10).

## 5. Conclusions

Millennial-scale events are a robust phenomenon of the Earth system. These events are most easily identifiable during glacial cycles. The events on time scales of 1–7 ka are discernible in North Atlantic  $\delta^{18}\text{O}$  records and the Vostok methane and deuterium records. Using a simple model of the seesaw mechanism we have shown that, with well-resolved data, it may be possible to simulate the high-latitude northern hemisphere temperatures during the glacial periods MIS 3, MIS 6 and MIS 8. In the absence of data which resolve millennial variability for the previous four glacial periods (excepting MIS 3 and perhaps MIS 8) this work should be regarded as a ‘proof of concept’ rather than a record of N. Hemisphere variability to be cited. We suggest that as higher resolution records become available the simple model presented here will be equally valid for MIS 10 and earlier periods. The new high-resolution records from the European Project of Ice Coring in Antarctica (EPICA) will be particularly useful to test the procedure that we have outlined in this paper. The record from Dome C, Station Concordia will cover at least four glacial cycles during times of stronger obliquity signal before 400 ka BP. On the other hand, the ice core from Dronning Maud Land is the first deep inland ice core in the Atlantic sector of Antarctica where we expect a stronger signal of the thermal-bipolar seesaw. This provides an opportunity to better test this simple but compelling concept.

Multiple characteristics of the millennial events during the glacial periods are closely matched to parallel events during MIS 3, particularly during MIS 6 and MIS 8. The fact that these events are identifiable in existing records of Antarctic ice sheets and North Atlantic marine cores, offers a potentially useful aid to the synchronisation of these records. The precision of this method of synchronisation is presently hampered by the lack of continuous high-resolution sampling in both ice cores and ocean sediment and uncertainty in the gas-ages of the Vostok ice core. Nevertheless the sections of each record that have been sampled in higher resolution show promise and indicate that the millennial-scale events may eventually be useful for the synchronisation of these records, potentially as long ago as 1 Ma (EPICA community members, 2004).

## Acknowledgements

We remember gratefully Nick Shackleton’s stimulating seminar which he delivered at the University of Bern on November 21, 2005. His concern was the consistent combination of high-resolution marine sedimentary data with the emerging record from the EPICA Dome Concordia ice core. We are thankful for his enthusiasm and strong support for polar ice core research and paleoclimate modelling. Nick’s ideas and approaches expressed during his seminar in Bern were the basis of planned further collaboration. We are saddened by the

thought that Nick will no longer guide this effort. Mark Siddall holds a postdoctoral position funded by the European STOPFEN European Network re-search project (HPRN-CT-2002-00221). Support from the Swiss National Science Foundation and the University of Bern is acknowledged. This is IPRC contribution #380.

## References

- Alley, R.B., Marotzke, J., Nordhaus, W.D., Overpeck, J.T., Peteet, D.M., Pielke Jr., R.A., Pierrehumbert, R.T., Rhines, P.B., Stocker, T.F., Talley, L.D., Wallace, J.M., 2003. Abrupt climate change. *Science* 299, 2005–2010.
- Bacon, M.P., Anderson, R.F., 1982. Distribution of thorium isotopes between dissolved and particulate forms in the deep-sea. *Journal of Geophysical Research—Oceans and Atmospheres* 87, 2045–2056.
- Bard, E., 2002. Climate shock: abrupt changes over millennial time scales. *Physics Today* 55, 32–37.
- Bard, E., Rostek, F., Turon, J.-L., Gendreau, S., 2000. Hydrological impact of Heinrich events in the subtropical northeast Atlantic. *Science* 289, 1321–1324.
- Bender, M., Sowers, T., Dickson, M.-L., Orchardo, J., Grootes, P., Mayewski, P.A., Meese, D.A., 1994. Climate correlations between Greenland and Antarctica during the past 100,000 years. *Nature* 372, 663–666.
- Blunier, T., Brook, E., 2001. Timing of millennial-scale climate change in Antarctica and Greenland during the last glacial period. *Science* 291, 109–112.
- Blunier, T., Schwander, J., Stauffer, B., Stocker, T., Dašljenbach, A., Indermuhle, A., Tschumi, J., Chappellaz, J., Raynaud, D., Barnola, J.-M., 1997. Timing of the Antarctic cold reversal and the atmospheric CO<sub>2</sub> increase with respect to the younger Dryas event. *Geophysical Research Letters* 24, 2683–2686.
- Blunier, T., Chappellaz, J., Schwander, J., Dällenbach, A., Stauffer, B., Stocker, T., Raynaud, D., Jouzel, J., Clausen, H.B., Hammer, C.U., Johnsen, S.J., 1998. Asynchrony of Antarctica and Greenland climate during the last glacial. *Nature* 394, 739–743.
- Broecker, W.S., 1987. The biggest chill. *Natural History* 96 (10), 74.
- Broecker, W.S., 1998. Paleocean circulation during the last deglaciation: a bipolar seesaw? *Paleoceanography* 13 (2), 119–121.
- Bryan, K., Manabe, S., Pacanowski, R.C., 1975. Global ocean-atmosphere climate model. 2. Oceanic circulation. *Journal of Physical Oceanography* 5 (1), 30–46.
- Chappellaz, J., Blunier, T., Raynaud, D., Barnola, J.M., Schwander, J., Stauffer, B., 1993. Synchronous changes in atmospheric CH<sub>4</sub> and Greenland climate between 40 and 8 ka BP. *Nature* 366, 443–445.
- CLIMAP Project Members, 1984. The last interglacial ocean. *Quaternary Research* 21, 123–224.
- Collins, W.D., Bitz, C.M., Blackmon, M.L., Bonan, G.B., Bretherton, C.S., Carton, J.A., Chang, P., Doney, S.C., Hack, J.J., Henderson, T.B., Kiehl, J.T., Large, W.G., McKenna, D.S., Santer, B.D., Smith, R.D., 2005. The community climate system model: CCSM3. *Journal of Climate*, in press.
- Crowley, T.J., 1992. North Atlantic deep water cools the southern hemisphere. *Paleoceanography* 7, 489–497.
- Dansgaard, W., Johnsen, S.J., Clausen, H.B., Dahl-Jensen, D., Gundestrup, N., Hammer, C.U., Oeschger, H., 1984. North Atlantic climatic oscillations revealed by deep Greenland ice cores. In: Hansen, J.E., Takahashi, T. (Eds.), *Climate Processes and Climate Sensitivity*, Geophysical Monograph Series, vol. 29. AGU, Washington DC, pp. 288–298.
- Dansgaard, W., Johnsen, S.J., Clausen, H.B., Dahl-Jensen, D., Gundestrup, N.S., Hammer, C.U., Hvidberg, C.S., Steffensen, J.P., Sveinbjornsdottir, A.E., Jouzel, J., Bond, G., 1993. Evidence for general instability of past climate from a 250-ka ice-core record. *Nature* 364, 218–220.
- Delmotte, M., Chappellaz, J., Brook, E., Yiou, P., Barnola, J.M., Goujon, C., Raynaud, D., Lipenkov, V.I., 2004. Atmospheric methane during the last four glacial-interglacial cycles: rapid changes and their link with Antarctic temperature. *Journal of Geophysical Research* 109, D12104.
- EPICA Members, 2004. Eight glacial cycles from an Antarctic ice core. *Nature* 429, 623–628.
- Gildor, H., Tziperman, E., 2000. Sea ice as the glacial cycles' climate switch: role of seasonal and orbital forcing. *Paleoceanography* 15 (6), 605–615.
- Hemming, S.R., 2004. Heinrich events: massive late Pleistocene detritus layers of the North Atlantic and their global climate impact. *Review of Geophysics* 42, RG1005.
- Honeyman, B.D., Balistrieri, L.S., Murray, J.W., 1988. Oceanic trace-metal scavenging—the importance of particle concentration. *Deep-Sea Research Part 1* 35 (2), 227–246.
- Imbrie, J., McIntyre, A., Mix, A.C., 1984. Oceanic response to orbital forcing in the late quaternary: observational and experimental strategies. In: Berger, A., Schneider, S.H., Duplessy, J.-C. (Eds.), *Climate and Geosciences, A Challenge for Science and Society in the 21st Century*. D. Reidel Publishing Company, Dordrecht.
- Johns, T.C., Gregory, J.M., Ingram, W.J., Johnson, C.E., Jones, A., Lowe, J.A., Mitchell, J.F.B., Roberts, D.L., Sexton, D.M.H., Stevenson, D.S., Tett, S.F.B., Woodage, M.J., 2003. Anthropogenic climate change for 1860 to 2100 simulated with the HadCM3 model under updated emissions scenarios. *Climatic and Dynamics* 20, 583–612.
- Knutti, R., Flückiger, J., Stocker, T.F., Timmermann, A., 2004. Strong hemispheric coupling of glacial climate through freshwater discharge and ocean circulation. *Nature* 430, 851–856.
- Lambeck, K., Chappell, J., 2001. Sea level change through the last glacial cycle. *Science* 292 (5517), 679–686.
- Lorenz, E.N., 1963. Deterministic nonperiodic flow. *Journal of the Atmospheric Sciences* 20 (2), 130–141.
- Manabe, S., Bryan, K., Spelman, M.J., 1975. Global ocean-atmosphere climate model. 1. Atmospheric circulation. *Journal of Physical Oceanography* 5 (1), 3–29.
- McManus, J.F., Oppo, D.W., Cullen, J.L., 1999. A 0.5-million-year record of millennial-scale climate variability in the North Atlantic. *Science* 283 (5404), 971–975.
- Müller, S.A., Joos, F., Edwards, N.R., Stocker, T.F. Water mass distribution and ventilation time scales in a cost-efficient, 3-dimensional ocean model. *Journal of Climate*, in press.
- North Greenland Ice Core Project members, 2004. High-resolution record of Northern Hemisphere climate extending into the last interglacial period. *Nature* 431, 147–151.
- Nürnberg, D., 1995. Magnesium in tests of neogloboquadrina-pachyderma sinistral from high northern and southern latitudes. *Journal of Foraminiferal Research* 25 (4), 350–368.
- Oeschger, H., Siegenthaler, U., Schotterer, U., Gugelmann, A., 1975. Box diffusion-model to study carbon-dioxide exchange in nature. *Tellus* 27 (2), 168–192.
- Oeschger, H., Beer, J., Siegenthaler, U., Stauffer, B., Dansgaard, W., Langway, C.C., 1984. Late glacial climate history from ice cores. In: Hansen, J.E., Takahashi, T. (Eds.), *Climate Processes and Climate Sensitivity*, Geophysical Monograph Series, vol. 29. AGU, Washington DC, pp. 299–306.
- Oppo, D.W., McManus, J.F., Cullen, J.L., 1998. Abrupt climate events 500,000 to 340,000 years ago: evidence from subpolar north Atlantic sediments. *Science* 279 (5355), 1335–1338.
- Oxford English Dictionary Online, 2005. <<http://dictionary.oed.com/>>, Oxford University Press, Oxford.
- Paillard, D., Parrenin, F., 2004. The Antarctic ice sheet and the triggering of deglaciations. *Earth and Planetary Science Letters* 227 (3–4), 263–271.
- Pailler, M., Bard, E., 2002. High-frequency paleoceanographic changes during the past 140,000 years recorded by the organic matter in

- sediments off the Iberian Margin. *Paleogeography, Paleoclimatology, Paleoecology* 181, 431–452.
- Petit, J.R., Jouzel, J., Raynaud, D., Barkov, N.I., Barnola, J.M., Basile, I., Bender, M., Chappellaz, J., Davis, M., Delaygue, G., Delmotte, M., Kotlyakov, V.M., Legrand, M., Lipenkov, V.Y., Lorius, C., Pepin, L., Ritz, C., Saltzman, E., Stievenard, M., 1999. Climate and atmospheric history of the past 420,000 years from the Vostok ice core, Antarctica. *Nature* 399 (6735), 429–436.
- Rohling, E.J., Palike, H., 2005. Centennial-scale climate cooling with a sudden cold event around 8,200 years ago. *Nature* 434 (7036), 975–979.
- Schmittner, A., Saenko, O.A., Weaver, A.J., 2003. Coupling of the hemispheres in observations and simulations of glacial climate change. *Quaternary Science Reviews* 22, 659–671.
- Shackleton, N.J., Hall, M.A., 2000. Phase relationships between millennial-scale events 64,000–24,000 years ago. *Paleoceanography* 15 (6), 565–569.
- Siddall, M., Rohling, E.J., Almogi-Labin, A., Hemleben, Ch., Meischnner, D., Schmelzer, I., Smeed, D.A., 2003. Sea-level fluctuations during the last glacial cycle. *Nature* 423, 853–858.
- Spahni, R., Schwander, J., Flückiger, J., Stauffer, B., Chappellaz, J., Raynaud, D., 2003. The attenuation of fast atmospheric CH<sub>4</sub> variations recorded in polar ice cores. *Geophysical Research Letters* 30 (11), 1571.
- Steig, E.J., Alley, R.B., 2002. Phase relationships between Antarctica and Greenland climate records. *Annals of Glaciology* 35, 451–456.
- Stocker, T.F., 1998. The seesaw effect. *Science* 282, 61–62.
- Stocker, T.F., Johnsen, S.J., 2003. A minimum model for the bipolar seesaw. *Paleoceanography* 18 (1087).
- Stocker, T.F., Knutti, R., 2003. Do simplified models have any useful skill? *CLIVAR Exchanges* 8, 7–10.
- Stocker, T.F., Wright, D.G., Mysak, L.A., 1992. A zonally averaged, coupled ocean-atmosphere model for paleoclimate studies. *Journal of Climate* 5, 773–797.
- Stommel, H., 1961. Thermohaline convection with 2 stable regimes of flow. *Tellus* 13 (2), 224–230.
- Stommel, H., Arons, A.B., 1960. On the abyssal circulation of the world ocean. 2. An idealized model of the circulation pattern and amplitude in oceanic basins. *Deep-Sea Research* 6 (3), 217–233.
- Tarasov, L., Peltier, W.R., 2004. A geophysically constrained large ensemble analysis of the deglacial history of the North American ice-sheet complex. *Quaternary Science Reviews* 23 (3–4), 359–388.
- Webster's online English Dictionary, 2005. <<http://www.m-w.com/>>. Merriam-Webster Incorporated.